arXiv:2505.02787v1 [cs.CV] 5 May 2025

UNSUPERVISED TRAINING OF KEYPOINT-AGNOSTIC DESCRIPTORS FOR FLEXIBLE RETINAL IMAGE REGISTRATION

A PREPRINT

David Rivas-Villar[*1,2], **Álvaro S. Hervella**[†1,2], **José Rouco** [‡1,2], **and Jorge Novo**[§1,2]
[1]Grupo VARPA, Instituto de Investigacion Biomédica de A Coruña (INIBIC), Universidade da Coruña, 15006 A Coruña, Spain
[2]Departamento de Ciencias de la Computación y Tecnologías de la Información, Universidade da Coruña, A Coruña, 15071, A Coruña, Spain

ABSTRACT

Current color fundus image registration approaches are limited, among other things, by the lack of labeled data, which is even more significant in the medical domain, motivating the use of unsupervised learning. Therefore, in this work, we develop a novel unsupervised descriptor learning method that does not rely on keypoint detection. This enables the resulting descriptor network to be agnostic to the keypoint detector used during the registration inference.

To validate this approach, we perform an extensive and comprehensive comparison on the reference public retinal image registration dataset. Additionally, we test our method with multiple keypoint detectors of varied nature, even proposing some novel ones. Our results demonstrate that the proposed approach offers accurate registration, not incurring in any performance loss versus supervised methods. Additionally, it demonstrates accurate performance regardless of the keypoint detector used. Thus, this work represents a notable step towards leveraging unsupervised learning in the medical domain.

Keywords Medical image registration · Feature-based Registration · Retinal Image Registration · Medical Imaging

1 Introduction

Image registration is a vital task in modern healthcare, serving various clinical purposes such as enabling simultaneous analysis of images from different temporal revisions. However, manual alignment is impractical in the time-constrained clinical setting, necessitating automated registration methods.

In image registration, two images are aligned according to their visual content. A pair of images to register is composed of a fixed image, which generally remains unchanged, and a moving image, which is transformed to match the contents of the fixed image. These image pairs are usually from the same subject but captured with slight variations such as morphology changes (due to the passage of time or pathologies), different viewpoints, different lightning, etc. Therefore, the information contained in the images only partially overlaps.

Retinal Image Registration (RIR) is the process of matching and registering images of the retina following their content. Particularly, certain structures are specifically useful to register the images of the human retina. Specifically, the relevant structures include the blood vessels and optic disk, among others, while the background is usually discarded due to its homogeneity and lack of relevant landmarks.

There are multiple imaging techniques aimed at capturing images of the retina such as color fundus, OCT or fundus angiography. Applications using all of these modalities can take advantage of registration [1]. Among these, Color Fundus (CF) images are of particular relevance. This imaging method is very common, widespread, very cost effective [2], and can aid in diagnosing eye diseases as well as some systemic conditions.

[*]Corresponding author: david.rivas.villar@udc.es
[†]a.suarezh@udc.es
[‡]jrouco@udc.es
[§]jnovo@udc.es

CF registration is challenging due to three distinct factors. First, CF images are prone to multiple imaging defects, including blur, underexposure, overexposure, glares from light reflections, motion artifacts caused by gaze shifts, inconsistencies due to improper camera or subject placement, etc. Secondly, since CF images capture the retina, they exhibit unique characteristics specific to retinal imaging, such as the particular patterns relevant for registration (e.g., blood vessels), which render general medical image registration methods ineffective. Finally, morphological changes in the retina, such as the appearance or disappearance of blood vessels and the development of lesions (e.g., cotton wool spots), significantly alter the images' appearance and complicate the registration process.

Commonly, in medical imaging, classical registration approaches (i.e. those that do not use deep learning) have yielded the best results. Nowadays, deep learning methods provide similar or better results while having several advantages. Following a data driven learning approach, deep learning methods do not need to be manually tuned like classical approaches. This makes them preferable in terms of robustness and flexibility. However, one key disadvantage of most deep learning methods is their requirement of labeled data, which is markedly scarce in medical contexts. This specifically motivates the creation of unsupervised learning methods in the biomedical domain, which do not require labeled data.

Generally, current medical image registration methods are not keypoint-based, which makes them less effective for retinal images, particularly CF images. This is evidenced by the fact that the best-performing methods for CF registration are keypoint-based approaches, as any other approach fails to achieve the same performance due to, for instance, ineffective similarity metrics or unrealistic transformations. While deep learning-based registration methods are now predominant in this field, classical methods still achieve the best numerical results in this domain, despite their limitations [3]. The most effective deep learning methods currently involve complex pipelines, utilizing either supervised domain-specific detectors or detector-free techniques [4, 5].

We propose a straight-forward approach for unsupervised descriptor training that allows to use any arbitrary keypoint detector. This eliminates the dependency on labeled data and creates a detector-agnostic keypoint descriptor with all the advantages of deep learning (e.g. flexibility).

We test the unsupervised description network in combination with a series of representative detectors: classical keypoint detectors, anatomical features, and combinations of both, including novel detectors proposed in this work. Based on the experiments conducted on the public FIRE dataset, we conclude that our unsupervised descriptor network does not incur in any performance penalty versus its supervised counterpart, as it outperforms it. Moreover, we introduce a novel experimental setting to evaluate the trade-off between the number of keypoints and performance. The results show that our unsupervised descriptor network performs consistently well across all tested detectors, demonstrating its keypoint-agnostic properties. Crucially, our approach achieves competitive performance without relying on labeled data, addressing limitations of previous unsupervised methods and advancing the state of the art in this domain.

2 Related Work

Currently, CF registration is evaluated using the public benchmark dataset FIRE [6]. Among classical approaches, VOTUS [3] and REMPE [7] are notable. VOTUS is based on graphs from the arteriovenous tree, matching them using a novel algorithm and classical image features. It should be noted that VOTUS uses the transformation model with the most degrees of freedom in the state of the art. REMPE detects and matches both domain-specific keypoints and generic ones, optimizing matches with particle-swarm and RANSAC. It employs a specialized transformation model tailored to fundus images.

In terms of deep learning methods, multiple approaches obtain accurate performance. Current approaches can be divided into detector-based methods and detector-less ones (i.e. with or without keypoint detector). Importantly, unsupervised detector-based methods are, currently, unable to compete with the rest of the approaches in terms of results, despite their advantages. Notably, most of these methods use homographic transformations.

One of the most notable supervised detector-based methods is SuperRetina with Knowledge Distillation [8], which builds upon SuperRetina [5]. It leverages reverse knowledge distillation to train a heavier model, resulting in marginal performance improvements. The base SuperRetina [5] is itself adapted from SuperPoint [9]. SuperRetina jointly trains a detector and descriptor network using a ground truth of vessel keypoints. It introduces a keypoint-expansion module aimed at improving the supervised learning of keypoints, resulting in additional detections beyond those initially included in the ground truth.

A significant pitfall of SuperRetina and its derivative methods is their reliance on large amounts of keypoints. This was addressed on by ConKeD [4] and, later, ConKeD++ [10]. Whereas SuperRetina uses approximately 740 keypoints, ConKeD++ uses around 115 while producing equivalent results. This is beneficial due to the lower computational complexity associated with matching less descriptors and exploring less alternatives during transformation estimation as

well as the increased robustness. ConKeD is based on two separate networks, detector and descriptor. The supervised detector network detects domain specific keypoints, blood vessel crossovers and bifurcations. The descriptor network is trained using these detected keypoints with a novel multi-positive and multi-negative loss that improves performance and data efficiency. In particular, ConKeD++ improved the results of ConKeD by exploring a novel rank-wise contrastive loss, FastAP [11]. Importantly, it should be noted that both SuperRetina derivatives and ConKeD ones generate descriptors conditioned on the keypoints they detect, meaning that the descriptors cannot be used with other detectors.

The most relevant detector-less method for CF images is GeoFormer [12]. GeoFormer is based on the pipeline of LoFTR [13] which, using transformers, extracts dense matches from the image pair at coarse level and then refines the accurate matches to a finer level later on. GeoFormer [12] enhances this pipeline by incorporating RANSAC, improving the performance by considering both spatial and image similarity constraints.

Overall, none of these deep learning method reaches the performance level of classical methods (i.e. VOTUS [3]). However, it should be noted that classical approaches falter in category A, the most clinically relevant. In this work we intend to combine the advantages of both classical and deep learning approaches. By creating an unsupervised description network, we leverage the data-driven training of deep learning. This description network can then be combined with arbitrary keypoint detectors of multiple types (i.e. learned, classical or both) which are completely decoupled from the descriptors allowing easy domain adaptation.

3 Methodology

Our proposal builds upon the description approach of ConKeD++ [10]. However, instead of using a supervised keypoint detector to train the descriptors, we propose to randomly sample keypoints from the retinal fundus. This makes the resulting description network unsupervised and keypoint-agnostic (i.e. applicable to any arbitrary keypoint detector). In that line, we propose to use a set of representative keypoint detectors like anatomical keypoints (including those used in ConKed++), classical keypoints, and combinations of both, alongside our proposed description network.

After the computation of both keypoints and descriptors, the descriptors are matched and then, the paired keypoints, are used to estimate the transformation using RANSAC. It should be noted that, both the detection and description are carried out using an input image size of 565×565, making the obtained pipeline and results equivalent to ConKeD++. Importantly, our description network can be trained with any arbitrary input image size. The transformation estimation through RANSAC is done in the original test set (FIRE) image size, enabling direct comparison with the state of the art. Like most of the state of the art methods, we use homographic transformations.

3.1 Unsupervised keypoint training

Our proposal for unsupervised descriptor learning builds upon the state of the art work ConKeD++. This method was devised to learn descriptors for particular keypoints (i.e. blood vessel crossovers and bifurcations) and relies on a supervised detection network to locate them. In this work, we propose UnConKeD (**Un**supervised **ConKeD**++), which extends ConKeD++ for unsupervised descriptor learning without any detector, eliminating the dependency on labeled data. Thus, the description network is keypoint-agnostic meaning that it can work with any arbitrary keypoint detector. An overview of the training methodology can be seen in Figure 1.

We take advantage of the multi-view batch proposed in ConKeD containing multiple views (i.e. augmentations) of the same original image (1 original image and N extra views). However, while in the original ConKeD and ConKeD++ the keypoints are sampled from the images following the inference of a supervised detector network (thus dependent on labeled data), in UnConKeD we propose to sample keypoints randomly from the RoI (Region of Interest) of the original image. This modification serves two primary purposes: firstly, it eliminates the dependency on labeled data, and secondly, it enables the framework to learn descriptors for any arbitrary keypoint on the retinal surface. Following the keypoint sampling, the network generates dense local descriptor maps associated to each pixel position for each image in the batch. Subsequently, descriptors corresponding to the sampled keypoints are selected to compute the loss. Following ConKeD++, we use Fast AP loss [10, 11].

A key difference between the ConKeD approach and our proposal is the number of sampled keypoints used in training. As ConKeD uses a detector network, the number of keypoints is limited by the vascular structure of the retina. In the proposed approach, the keypoints are freely sampled from the RoI, that is, keypoints are not constrained by morphological structures. Therefore, our approach always samples a fixed amount of keypoints, removing randomness from the training as we can arbitrarily set the number of sampled keypoints. Furthermore, as we remove any dependency on supervision, we can use any dataset, with or without labels. All these improvements speed up the training process as the network receives more and, potentially, better and more diverse feedback in each batch. However, our approach also has some disadvantages. Randomly sampling keypoints in CF images means that many low-interest background

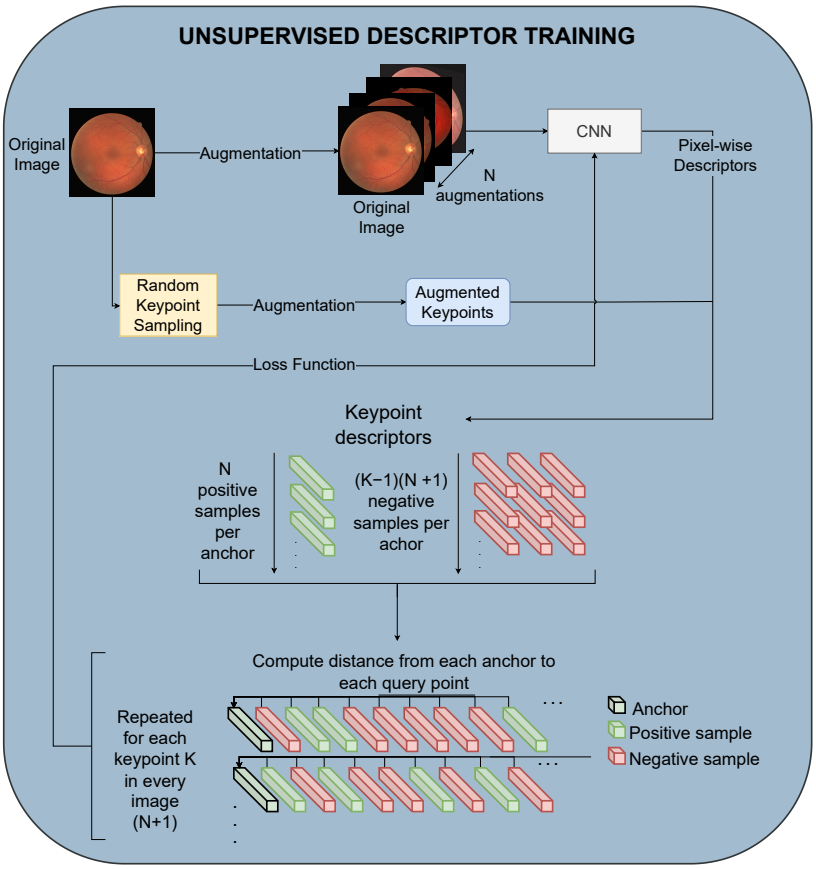

Figure 1: Proposed unsupervised descriptor training

points are going to be sampled (due to the amount of area that is background versus relevant areas). While a portion of background points may be discernible from others due to proximity to actual landmarks, some of them will inevitably be unreliable low-discriminativity points. Although this may slow convergence, improvements in keypoint sampling and dataset flexibility help compensate.

3.2 Keypoint detection

In this proposal we explore different alternatives for keypoint detection by leveraging the unsupervised keypoint-agnostic descriptor network, enabling different variants of our methodology and providing a comprehensive comparison among them. In particular, we propose to test the following methods:

Random Keypoints. As baseline, we propose to use random keypoints by generating a grid of equispaced points. Due to differences in image content, these keypoints appear in varying positions across registration pairs, resulting in a structured yet random distribution within the retina.

Classic keypoint detectors. These detectors have been successfully used in multiple applications even if they are mostly substituted by deep learning-based ones nowadays. We have selected the following commonly used approaches:

- SIFT (Scale-Invariant Feature Transform) [14]: detects keypoints at multiple scales and orientations, using a Gaussian pyramid and difference of Gaussians. These keypoints are then filtered in subsequent steps.
- Harris corner detector [15]: identifies corners by measuring local intensity variations in different directions.
- FAST (Features from Accelerated Segment Test) corner detector [16]: works by analyzing a circle of pixels around each candidate pixel. If sufficient pixels are different than the candidate pixel, it is classified as a corner.
- ORB (Oriented FAST and Rotated BRIEF) [17]: a modified version of FAST, which filters keypoints using the Harris corner measure.

- CenSurE (Center Surround Extremas) [18]: detects local extrema using center-surround difference-of-Gaussian filters, simulated with octagons. For greater accuracy, we use the STAR approach, which simulates them using circles.

Blood vessel crossovers and bifurcations. These domain specific keypoints have proven to be highly accurate and capable of enabling successful registration in ConKeD [4, 10].

Blood vessel segmentations. We segment the blood vessels in CF images using a state of the art network [19]. Using the entire blood vessels, as opposed to discrete points like crossovers and bifurcations, can improve the results since the vessels are distributed along the retinal surface, unlike the crossovers and bifurcations. This approach has not been tested in the state of the art, possibly due to the large number of keypoints from segmentation which increases computational costs. To address this, we propose reducing the keypoints using methods like morphological skeletonization or Canny edge detection.

Classic keypoint detectors over blood vessel segmentation logits. We propose using the logits from the vessel segmentation network as input for classic keypoint detector methods, as this pre-processed data could enhance their performance. This approach remains untested in the state of the art.

3.3 Training details

To train the descriptor network we follow the reference ConKeD++ [10] methodology. Thus, we employ the same network and input image size. In particular, the network is trained from scratch for 1000 epochs with Adam [20] as the optimizer with a fixed learning rate of $1e-4$. The number of bins used in the FastAP Loss, was set to $Q = 10$. To train, we use the Messidor-2 dataset [21, 22], normalizing image size to 565×565 (ConKeD++ input size). We also use the exact same augmentation regime used in ConKeD++. We use random affine transformations for spatial augmentations. These transformations include rotations of $\pm 60°$, translations of $0.25 \times imageSize$ in each axis, scaling between $0.75 - 1.25 \times imageSize$ and shearing of $\pm 30°$. For color augmentation, we use random changes in the HSV color space and Gaussian noise (mean 0, standard deviation 0.05), with noise applied 25% of the time. Both spatial and HSV augmentations are applied to every augmented image in the batch. Each batch is composed of 1 original image and N augmentations which, following ConKeD++, means a batch of 10 images, 9 of which are augmented. Leveraging the controlled sampling process, from each image we selected the maximum amount of keypoints that our hardware setup allows for, 1460 for each image. In this regard, the training was carried out using two Nvidia A100, each with 80 GB of VRAM.

3.4 Matching details

Increasing efficiency in detector-based registration pipelines invariably involves reducing the number of keypoints, which decreases comparisons during descriptor matching and the number of possible combinations in transformation estimation. Thus, finding keypoint detectors with the best performance-per-detected-keypoint is desirable. We propose to evaluate the keypoint detectors on a predefined set amounts of detected keypoints, allowing for direct performance comparison. We propose to average the number of keypoint detections over the test set and modify the different sensitivity parameters in the keypoint detectors such that the methods detect these specific numbers of keypoints. We propose to use 100, 500, 1000 and unlimited keypoints (removing any threshold). For random keypoints, we use limits of 100, 500, 1000, and an additional 5000, and 40000 to account for the expected lower performance.

The blood vessel crossovers and bifurcations detector herein tested is the same used in ConKeD++ [10], making the results directly comparable.

3.5 Datasets and evaluation

To train the unsupervised description network we use the Messidor-2 dataset [21, 22], which consits of 1748 images captured in a set of Diabetic Retinopathy examinations. The images are captured using a 45º of FOV. For evaluation, we use the FIRE dataset, which is the only one with suitable ground truth for CF registration. It contains 129 retinal images from 39 patients, generating 134 registration pairs. The dataset is divided into three categories: Category S (71 pairs) with high overlap, Category P (49 pairs) with low overlap, and Category A (14 pairs) with high overlap and disease progression, making it particularly challenging and highly clinically relevant. We evaluate the registration using the FIRE proposed metric, Registration Score, which must be computed at the dataset's original resolution [6]. Registration Score is based the Euclidean distance among the the ground truth of points. Plotting the average control point distance against a mobile error threshold allows us to calculate the Area Under the Curve (AUC) metric, which is the Registration Score.

FIRE Dataset	FIRE	A	P	S	Avg.	W. Avg.
CB + ConKeD++ [10]	0.760	0.766	0.503	0.945	0.738	0.765
CB + UnConKeD	0.769	0.757	0.513	0.948	0.739	0.769

Table 1: Comparison between the supervised and unsupervised descriptor training using crossovers and bifurcations as the keypoints

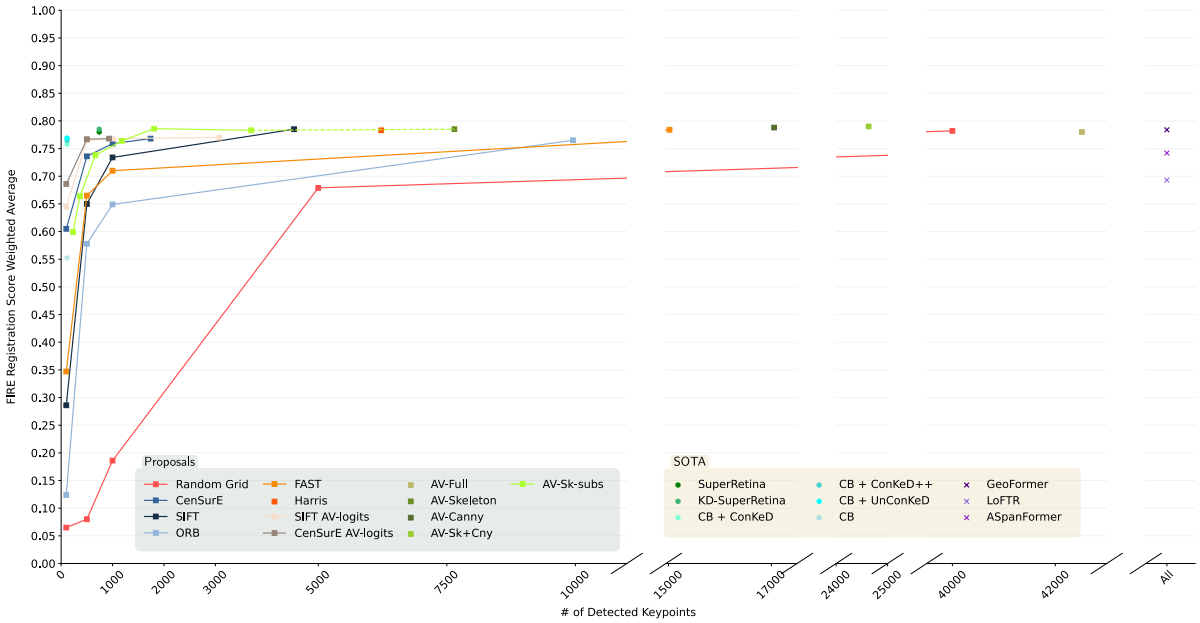

Figure 2: Results for the different keypoint detectors in FIRE, measured in Weighted Average of Registration Score AUC

4 Results and Discussion

4.1 Supervised vs Unsupervised descriptor training

The results for the evaluation comparing the performance of the supervised and unsupervised detector networks are shown in Table 1. In this table, we can see that, in comparison to ConKeD++, the unsupervised training slightly improves the performance. It is worth noting that this comparison is performed using vessel crossings and bifurcations as keypoints, and ConKeD++ has been specifically trained to produce descriptors for these keypoints, meaning it is the most favorable setup for ConKeD++. In this setting, even performance parity would be an achievement, and while the performance improvement is relatively modest, it represents a meaningful step forward in unsupervised learning.

The proposed random keypoint sampling strategy also has additional advantages at inference time, in addition to additional flexibility resulting from forgoing labeled data. In ConKeD++, the lack of feedback for non-crossover or bifurcation points can lead to inaccurate descriptors and incorrect matching, if any point other that those is mistakenly detected. In contrast, our approach trains with points from the entire retinal surface, enabling it to produce accurate descriptors for all retinal areas, improving its robustness. In summary, the unsupervised process introduces no drawbacks while offering significant benefits, particularly in the medical domain where the absence of supervised data is highly advantageous.

4.2 Keypoint detectors

The results of combining our unsupervised keypoint descriptor with different keypoint detectors are shown in Table 2. Moreover, the results are shown in a intuitive graphical visualization in Figure 2.

First, as a baseline, using the random keypoint grid with low numbers of keypoints is ineffective in producing useful results. The random keypoint grid performs competitively only with a large number of keypoints (40k), which is

FIRE Dataset	Average # of keypoints	FIRE	A	P	S	Avg.	W. Avg.
CB	115	0.769	0.757	0.513	0.948	0.739	0.769
Random Keypoint Grid	100	0.065	0.054	0.000	0.113	0.056	0.065
	500	0.080	0.071	0.007	0.132	0.070	0.080
	1,000	0.186	0.220	0.091	0.245	0.185	0.186
	5,000	0.679	0.731	0.458	0.822	0.670	0.679
	40,000	0.782	0.777	0.544	0.948	0.756	0.782
CENSURE	100	0.605	0.537	0.267	0.852	0.552	0.605
	500	0.736	0.734	0.460	0.926	0.707	0.736
	1,000	0.759	0.743	0.496	0.944	0.728	0.759
	1,740 (all)	0.767	0.766	0.518	0.940	0.741	0.767
ORB	100	0.124	0.203	0.048	0.161	0.137	0.124
	500	0.578	0.426	0.204	0.866	0.499	0.578
	1,000	0.649	0.537	0.296	0.915	0.583	0.649
	9,953 (all)	0.765	0.771	0.491	0.953	0.739	0.765
SIFT	100	0.286	0.251	0.131	0.400	0.261	0.286
	500	0.65	0.486	0.351	0.889	0.575	0.65
	1,000	0.734	0.723	0.441	0.938	0.701	0.734
	4,529 (all)	0.785	0.774	0.542	0.954	0.757	0.785
FAST	100	0.347	0.403	0.141	0.478	0.341	0.347
	500	0.664	0.637	0.349	0.888	0.625	0.664
	1,000	0.710	0.669	0.409	0.925	0.668	0.710
	15,020 (all)	0.784	0.771	0.544	0.952	0.756	0.784
Harris	6,224	0.783	0.777	0.541	0.950	0.756	0.783
AV All Points	42,518	0.780	0.780	0.523	0.958	0.754	0.780
AV Skeleton	7,648	0.785	0.783	0.538	0.956	0.759	0.785
AV Canny	17,054	0.788	0.786	0.548	0.955	0.763	0.788
AV Skelet+Canny	24,631	0.790	0.786	0.551	0.956	0.764	0.790
SIFT over AV logits	100	0.645	0.557	0.345	0.870	0.591	0.645
	500	0.765	0.760	0.509	0.943	0.737	0.765
	1,000	0.768	0.754	0.518	0.944	0.739	0.768
	3,079 (all)	0.770	0.757	0.517	0.946	0.740	0.77
CENSURE over AV logits	100	0.686	0.611	0.417	0.886	0.638	0.686
	500	0.767	0.734	0.518	0.945	0.732	0.767
	932 (all)	0.767	0.723	0.527	0.943	0.731	0.767
AV Skeleton Random Subsampling	3,696	0.783	0.777	0.533	0.957	0.756	0.783
	1,807	0.786	0.783	0.544	0.953	0.760	0.786
	1,182	0.764	0.766	0.507	0.941	0.738	0.764
	667	0.738	0.757	0.491	0.904	0.717	0.738
	366	0.664	0.637	0.425	0.834	0.632	0.664
	231	0.599	0.583	0.372	0.758	0.571	0.599

Table 2: Results in FIRE for the different keypoint detectors combined with the unsupervised descriptors, measured in Registration Score AUC.

impractical due to the high matching cost. However, this evaluation serves as a baseline for comparing with state of the art, as it is completely unsupervised, since the points are random.

The classical keypoint detectors offer accurate performance, specially at higher numbers of keypoints. ORB and SIFT require at least 500 keypoints to obtain accurate results. However, CenSurE surpasses 0.6 of AUC at just 100 keypoints. Furthermore, with 500 keypoints CenSurE reaches similar levels to the supervised crossovers and bifurcations. Utilizing more keypoints (e.g. 1000 or all possible) incurs in diminishing returns, as the results do not improve sufficiently to justify the increase in keypoints used. Conversely, since ORB or SIFT exhibit lower performance with fewer keypoints, increasing the number of keypoints becomes more relevant in these methods. Interestingly, SIFT manages to improve

the results of CenSurE when using all detectable keypoints. However, this is simply due to SIFT detecting many more keypoints, (2.5×). This can also be intuitively seen in Figure 2.

In terms of corner detectors, FAST performs similarly to the keypoint detectors, positioning itself behind SIFT but ahead of ORB. FAST needs at least 500 keypoints to offer useful performance. Removing the sensitivity threshold, it detects around 15k corners, an impractically large number, which allows this method to compete with SIFT and CenSurE. In contrast, the Harris corner detector offers approximately the same performance but utilizing half of the keypoints, around 6k.

The different alternatives using keypoints derived from the arteriovenous tree are among the best-performing methods. Using all the keypoints in the vessel segmentations is not practical despite the good performance, as it results in more than 40k keypoints. The different strategies for reducing the amount of keypoints proved to be useful and reliable. Both using the Canny edge detector and morphological skeletonization massively reduce the amount of keypoints while keeping or even improving the performance. Regarding the comparison between both approaches, Canny provides double the number of keypoints than the skeleton for minuscule performance gains. Combining the Canny edges with the skeletonization marginally improves performance compared to using each method separately, while significantly increasing the keypoints. Thus, using the skeleton provides the best balance between performance and computational cost, as it uses around 7.5k keypoints. However, it is still possible to further improve the efficiency of this method, since, due to the structure of the blood vessels, many keypoints are redundant in the transformation estimation. Thus, we randomly sub-sample these keypoints. By iterating over the skeleton, we remove the closest neighbors of each point using increasingly big kernel sizes. The results of this approach can be seen in Table 2 under the name "AV Skeleton Sub-sampling". Using less than 25% of the original points (i.e. 1807 as opposed to 7648) we retain the performance while significantly reducing the computational cost. Therefore, this approach can be considered a good compromise between performance and cost, as it offers the best results despite using a limited number of keypoints.

Finally, applying keypoint detectors to the logits of the segmentation network improves performance compared to using the detectors directly on the images. However, this improvement is only relative the number of used keypoints, meaning it only improves the efficiency of the method allowing better results with less keypoints. Using the logits as input instead of the image causes CenSurE and SIFT detect less keypoints, which limits their top performance but the performance-per-detection improves. This can be easily seen in Figure 2 as the results of using logits as input for the detectors are more to the top and left than the detectors with images as input.

Overall, these results highlight the keypoint-agnostic nature of our unsupervised description network, as it is able to consistently produce accurate registrations with a wide variety of keypoint detectors.

4.3 State of the Art Comparison

In this subsection, we compare our approaches with methods from the state of the art. Direct comparisons can be seen in Table 3 as well as Figure 2.

Our unsupervised descriptor training, combined with vessel points, surpasses the results of all other deep-learning-based methods in the state of the art. The Canny approach produces the best overall metrics for all categories within deep learning methods except in category P. In this category, the best deep learning approach is GeoFormer. However, it should be noted that this method evaluates using an incomplete set of images. The sub-sampled skeleton approach, which has significantly less keypoints, obtains the second best performance across all deep learning methods. Importantly, both of these approaches, Canny and sub-sampled skeleton, obtain the best results among all methods in category A, the one that holds the most clinical significance due to its pathological progression.

While CenSurE with AV Logits ranks slightly lower, its performance remains remarkable as it utilizes only 500 keypoints. It uses fewer keypoints than any other method outperforming it.

Another interesting comparison to make is between detector-less methods and the random keypoint approach. Detector-less methods such as GeoFormer [12] can be, effectively, unsupervised. However, they use the whole image to obtain matches which is, potentially, more computationally intensive. A direct comparison for these methods would be the random keypoint grid which is fully unsupervised as the keypoints are not generated based on any image feature or learning process. In this regard, our random grid approach using 40k points obtains a weighted registration score of 0.782, which is comparable to the 0.784 from Geoformer. For reference, there are a approximately 215k points in the RoI of the FIRE fundus images at the operating resolution of our description network. Furthermore, Geoformer operates at a higher resolution meaning that it can create finer matches but at higher computational cost.

Finally, the variants of our method using classical keypoint detectors considerably outperform previous methods using the same type of detectors [23, 24], (e.g. our Harris vs Harris+PIIFD [23] generates a performance increase of over

FIRE Dataset	FIRE	A	P	S	Avg.	W. Avg.
Classical						
VOTUS [3]	**<u>0.812</u>**	**0.681**	**<u>0.672</u>**	0.934	**0.762**	**<u>0.811</u>**
REMPE [7]	0.773	0.66	0.542	**<u>0.958</u>**	0.72	0.774
Harris-PIIFD [7, 23]	0.553	0.443	0.09	0.9	0.478	0.556
SURF+WGTM [7, 24]	0.472	0.069	0.061	0.835	0.322	0.472
Deep Learning						
AV Canny	***0.788***	***<u>0.786</u>***	*0.548*	***0.955***	***<u>0.763</u>***	***0.788***
AV Skeleton SubSampled	*0.786*	*0.783*	*0.544*	*0.953*	*0.760*	*0.786*
KD-SuperRetina [8]	-	0.783	0.558*	0.942	0.761*	0.785*
GeoFormer [12]	-	0.760	**0.559***	0.944	0.754*	0.784*
SuperRetina [5]	-	0.783	0.542*	0.94	0.755*	0.780*
CenSurE AV Logits 500	*0.767*	*0.734*	*0.518*	*0.945*	*0.732*	*0.767*
ConKeD++ [10]	0.760	0.766	0.503	0.945	0.738	0.765
ConKeD [4]	0.758	0.749	0.489	0.945	0.728	0.758
ASpanFormer [12]	-	0.703	0.495*	0.921	0.706*	0.742*
LoFTR [12]	-	0.711	0.359*	0.92	0.663*	0.693*
Retina-R2D2 [25]	0.695	0.726	0.352	0.925	0.645	0.575
Rivas-Villar [26]	0.657	0.660	0.293	0.908	0.620	0.552

Table 3: Comparison of our proposals (italics) with state-of-the-art methods, sorted by FIRE weighted average. Best results for each category in bold, best overall underlined. * indicates evaluation without the full set of images.

20%). Thus, we can conclude that our unsupervised descriptor is able to significantly boost the performance of classical detectors.

5 Conclusion

In this work, we present a novel unsupervised method for training keypoint descriptors. It addresses one of the main limiting factors of current learning approaches, the requirement for labeled data, which is specially scarce in the medical domain. Using random keypoint sampling from the retinal RoI, we create an unsupervised description network that is agnostic to keypoint detectors. In this sense, we test our approach with multiple representative keypoint detectors, including novel ones proposed in this work.

We empirically show that our unsupervised descriptor not only avoids a performance decrease compared to supervised training, but actually improves upon it. This eliminates the typical performance penalty of self-supervised or unsupervised methods. Furthermore, its consistently accurate performance across various keypoint detectors highlights its flexibility and keypoint-agnostic nature. Notably, when combined with several of our proposed keypoint detectors, our pipeline achieves competitive performance with current SOTA, even surpassing it. Our work represents a significant advancement that enables unsupervised methods to perform on par with or surpass supervised approaches, a crucial feat in medical fields.

References

[1] David Rivas-Villar, Alice R. Motschi, Michael Pircher, Christoph K. Hitzenberger, Markus Schranz, Philipp K. Roberts, Ursula Schmidt-Erfurth, and Hrvoje Bogunović. Automated inter-device 3d oct image registration using deep learning and retinal layer segmentation. *Biomed. Opt. Express*, 14(7):3726–3747, Jul 2023.

[2] Ra Ho, Lina D. Song, Jin A. Choi, and Donghyun Jee. The cost-effectiveness of systematic screening for age-related macular degeneration in south korea. *PLOS ONE*, 13(10):1–14, 10 2018.

[3] D. Motta, W. Casaca, and A. Paiva. Vessel optimal transport for automated alignment of retinal fundus images. *IEEE Transactions on Image Processing*, 28(12):6154–6168, 2019.

[4] David Rivas-Villar, Álvaro S. Hervella, José Rouco, and Jorge Novo. Conked: multiview contrastive descriptor learning for keypoint-based retinal image registration. *Medical & Biological Engineering & Computing*, 62(12):3721–3736, Dec 2024.

[5] Jiazhen Liu, Xirong Li, Qijie Wei, Jie Xu, and Dayong Ding. Semi-supervised keypoint detector and descriptor for retinal image matching. In Shai Avidan, Gabriel Brostow, Moustapha Cissé, Giovanni Maria Farinella, and Tal Hassner, editors, *Computer Vision – ECCV 2022*, pages 593–609, Cham, 2022. Springer Nature Switzerland.

[6] Carlos Hernandez-Matas, Xenophon Zabulis, Areti Triantafyllou, Panagiota Anyfanti, Stella Douma, and Antonis Argyros. Fire: Fundus image registration dataset. *Journal for Modeling in Opthalmology*.

[7] C. Hernandez-Matas, X. Zabulis, and A. A. Argyros. Rempe: Registration of retinal images through eye modelling and pose estimation. *IEEE Journal of Biomedical and Health Informatics*, 24(12):3362–3373, 2020.

[8] Sahar Almahfouz Nasser, Nihar Gupte, and Amit Sethi. Reverse knowledge distillation: Training a large model using a small one for retinal image matching on limited data. In *Proceedings of the IEEE/CVF Winter Conference on Applications of Computer Vision (WACV)*, pages 7778–7787, January 2024.

[9] Daniel DeTone, Tomasz Malisiewicz, and Andrew Rabinovich. Superpoint: Self-supervised interest point detection and description. In *Proceedings of the IEEE Conference on Computer Vision and Pattern Recognition (CVPR) Workshops*, June 2018.

[10] David Rivas-Villar, Álvaro S Hervella, José Rouco, and Jorge Novo. Conked++ - improving descriptor learning for retinal image registration: A comprehensive study of contrastive losses. *arXiv preprint arXiv:2404.16773*, 2024.

[11] Fatih Cakir, Kun He, Xide Xia, Brian Kulis, and Stan Sclaroff. Deep metric learning to rank. In *Proceedings of the IEEE/CVF Conference on Computer Vision and Pattern Recognition (CVPR)*, June 2019.

[12] Jiazhen Liu and Xirong Li. Geometrized transformer for self-supervised homography estimation. In *Proceedings of the IEEE/CVF International Conference on Computer Vision (ICCV)*, pages 9556–9565, October 2023.

[13] Jiaming Sun, Zehong Shen, Yuang Wang, Hujun Bao, and Xiaowei Zhou. Loftr: Detector-free local feature matching with transformers. In *Proceedings of the IEEE/CVF conference on computer vision and pattern recognition*, 2021.

[14] David G. Lowe. Distinctive image features from scale-invariant keypoints. *International Journal of Computer Vision*, 60(2):91–110, Nov 2004.

[15] C. Harris and M. Stephens. A combined corner and edge detector. In *Proceedings of the Alvey Vision Conference*, pages 23.1–23.6. Alvety Vision Club, 1988. doi:10.5244/C.2.23.

[16] Edward Rosten and Tom Drummond. Machine learning for high-speed corner detection. In Aleš Leonardis, Horst Bischof, and Axel Pinz, editors, *ECCV 2006*, pages 430–443, Berlin, Heidelberg, 2006. Springer Berlin Heidelberg.

[17] Ethan Rublee, Vincent Rabaud, Kurt Konolige, and Gary Bradski. Orb: an efficient alternative to sift or surf. pages 2564–2571, 11 2011.

[18] Motilal Agrawal, Kurt Konolige, and Morten Rufus Blas. Censure: Center surround extremas for realtime feature detection and matching. In David Forsyth, Philip Torr, and Andrew Zisserman, editors, *Computer Vision – ECCV 2008*, pages 102–115, Berlin, Heidelberg, 2008. Springer Berlin Heidelberg.

[19] Álvaro S. Hervella, José Rouco, Jorge Novo, and Marcos Ortega. Learning the retinal anatomy from scarce annotated data using self-supervised multimodal reconstruction. *Applied Soft Computing*, 91:106210, 2020.

[20] Diederik Kingma and Jimmy Ba. Adam: A method for stochastic optimization. In *International Conference on Learning Representations (ICLR)*, 12 2015.

[21] Michael D. Abràmoff, James C. Folk, Dennis P. Han, Jonathan D. Walker, David F. Williams, Stephen R. Russell, Pascale Massin, Beatrice Cochener, Philippe Gain, Li Tang, Mathieu Lamard, Daniela C. Moga, Gwénolé Quellec, and Meindert Niemeijer. Automated Analysis of Retinal Images for Detection of Referable Diabetic Retinopathy. *JAMA Ophthalmology*, 131(3):351–357, 03 2013.

[22] Etienne Decencière, Xiwei Zhang, Guy Cazuguel, Bruno Lay, Béatrice Cochener, Caroline Trone, Philippe Gain, Richard Ordonez, Pascale Massin, Ali Erginay, Béatrice Charton, and Jean-Claude Klein. Feedback on a publicly distributed image database: The messidor database. *Image Analysis & Stereology*, 33(3):231–234, 2014.

[23] J. Chen, J. Tian, N. Lee, J. Zheng, R. T. Smith, and A. F. Laine. A partial intensity invariant feature descriptor for multimodal retinal image registration. *IEEE Transactions on Biomedical Engineering*, 57(7):1707–1718, 2010.

[24] Gang Wang, Zhicheng Wang, Yufei Chen, and Weidong Zhao. Robust point matching method for multimodal retinal image registration. *Biomedical Signal Processing and Control*, 19:68–76, 2015.

[25] David Rivas-Villar, Álvaro S. Hervella, José Rouco, and Jorge Novo. Joint keypoint detection and description network for color fundus image registration. *Quantitative Imaging in Medicine and Surgery*.

[26] David Rivas-Villar, Álvaro S. Hervella, José Rouco, and Jorge Novo. Color fundus image registration using a learning-based domain-specific landmark detection methodology. *Computers in Biology and Medicine*, 140:105101, 2022.